Available online at www.sciencedirect.com
ScienceDirect
Journal of Hazardous Materials 149 (2007) 460–464
Journal of Hazardous Materials
www.elsevier.com/locate/jhazmat

Detoxification reactions of sulphur mustard on the surface of zinc oxide nanosized rods

G.K. Prasad *, T.H. Mahato, Beer Singh, K. Ganesan, P. Pandey, K. Sekhar

Defence Research and Development Establishment, Jhansi Road, Gwalior, India

Received 9 February 2007; received in revised form 2 April 2007; accepted 3 April 2007
Available online 6 April 2007

Abstract

Detoxification reactions of sulphur mustard, a deadliest chemical warfare agent were studied on the surface of zinc oxide nanorods at room temperature ($32 \pm 2\,^{\circ}C$) and the data was compared with that of the bulk ZnO. Prior to the reaction, the nanorods of zinc oxide were synthesized by the hydrothermal method and subsequently characterized by XRD, SEM, TG, N_2 BET, FT-IR. The data revealed the formation of nanorods with diameter ranging from 100 nm to 500 nm with length in microns. Obtained nanomaterial along with bulk ZnO were tested as reactive sorbent for the detoxification of sulphur mustard. Reaction was monitored by GC-FID technique and the reaction products were characterized by GC–MS. Data explores the role of hydrolysis and elimination reactions in the detoxification of sulphur mustard and it also reveals that zinc oxide nanorods and bulk ZnO show the half lives of 8.48 h, 24.75 h in the first 12 h and 122.47 h, 177.29 h from 12 h to 48 h of the reaction.

Keywords: Sulphur mustard; Chemical warfare agent; Zinc oxide; Detoxification and hydrothermal method

1. Introduction

Application of nanosized inorganic oxide materials as reactive sorbents has been a promising approach for the decontamination of chemical warfare (CW) agents [1–4]. Strong adsorbability and enhanced reactivity towards the toxicants make them the potential materials for the decontamination applications. These intriguing properties within the above materials are expected to be aroused owing to the high surface area due to smaller particle size and the reactive sites tailored in the form of edge and corner defects, unusual lattice planes, etc. Most likely, these active sites react in a stoichiometric fashion, thereby rendering the adsorbed toxic agents to non-toxic ones and the reactions are analogous to their solution behaviour [5,2].

Recent investigations have explored the promising decontamination applications of nanosized metal oxides such as AP-MgO, AP-Al_2O_3 and AP-CaO [6–11]. They possessed enhanced chemical reactivity towards CW agents including sulphur mustard, which undergo hydrolysis and elimination reactions on the surface of nanoparticles and the same was illustrated by MAS-NMR data. Especially sulphur mustard reacts with AP-MgO, AP-Al_2O_3 and AP-CaO with half lives of 17.8 h, 6.3 h and 8.5 h, respectively, at room temperature yielding the non-toxic elimination and hydrolysis products [12–15]. Although, they have the capability to decontaminate CW agents within few hours of duration, the search for newer and more efficient materials is still going on to ensure the preparedness and enhance the confidence levels regarding safety against the CW agents.

On the other hand, ZnO nanomaterials were found to have interesting applications such as surface acoustic wave filters [16], photonic crystals [17], light emitting diodes [18], photo detectors [19], varistors [20], gas sensors [21], solar cells [23] and catalysts. Recently, one of the variants of ZnO nanomaterials, i.e., ZnO nanorods (ZnO NR) have been synthesized by the hydrothermal method and were used for sensing [22] and catalytic applications [24]. Similar materials have also been used for the decontamination of dimethyl methyl phosphonate (DMMP), a well-known simulant for nerve agents [24,25]. Inspired by these applications, we have attempted to study the decontamination reaction of sulphur mustard (HD) on the surface of ZnO nanorods. After their synthesis, the sample was characterized by SEM, XRD, TG, FT-IR, N_2 BET and then the reactions were monitored by GC and the reaction products were characterized by GC–MS.

* Corresponding author.
E-mail address: gkprasad@lycos.com (G.K. Prasad).

0304-3894/$ – see front matter © 2007 Elsevier B.V. All rights reserved.
doi:10.1016/j.jhazmat.2007.04.010

2. Experimental

2.1. Materials

Zinc nitrate hexahydrate, hexamethylenetetramine (HMTA), acetonitrile, chloroform and ZnO were obtained from S.D. Fine Chemicals India Pvt. Ltd. Sulphur mustard of 99% (GC assay) purity was synthesized in our laboratory.

2.2. Characterization

XRD patterns were obtained in an X Pert Pro Diffractometer, Panalytical, Netherlands, using Cu Kα radiation. SEM investigations were carried out on a Philips instrument. N_2 BET measurements were done on Autosorb 1C of Quantachrome, USA make. Subsequently, thermograms were recorded on TGA-2950, TA instruments, USA and the IR data was acquired on Perkin-Elmer FT-IR (Model 1720X) of USA. The Nucon 5700 gas chromatograph equipped with FID detector and OV 17 column (30 m length, 0.5 mm i.d.) was used for the degradation kinetics of HD. Whereas, HP Agilent GC–MS system (5973 Inert) was used for the characterization of reaction products.

2.3. Synthesis of zinc oxide nanorods

Prior to the reaction studies, the zinc oxide nanorods were synthesized by the hydrothermal method as per a reported procedure [26]. For this purpose, the aqueous solution of zinc nitrate was added to the hexamethylene tetramine solution in a conventional reaction flask equipped with a reflux condenser. The reaction temperature was maintained at 98 °C and the reaction was continued for 20 h. Thereafter, the obtained materials were filtered and washed meticulously with ultrapure water. Subsequently, the material was dried at room temperature overnight and at 50 °C for 4 h. Obtained materials, ZnO nanorods along with bulk ZnO were used to study the reaction with HD at room temperature (32 ± 2 °C).

2.4. Reaction of sulphur mustard with ZnO nanorods

For this purpose, 100 μL of chloroform solution having 5 μL of HD was added to 300 mg of the above aggregate powder and the remaining HD was extracted by 5.0 mL of acetonitrile at periodic intervals of time until 48 h to study the kinetics of degradation on the surface of ZnO NR. Thereafter, the extracted solutions were analyzed by GC-FID at isothermal conditions at 110 °C and then the reaction products were characterized by GC–MS.

3. Results and discussion

Hydrothermal treatment of the aqueous solutions composed of zinc nitrate and hexamethylene tetramine at 98 °C facilitated the formation of ZnO nanorods. Formed nanorods were characterized by scanning electron microscopy and the electron micrographs are shown in Fig. 1a and b. The morphology

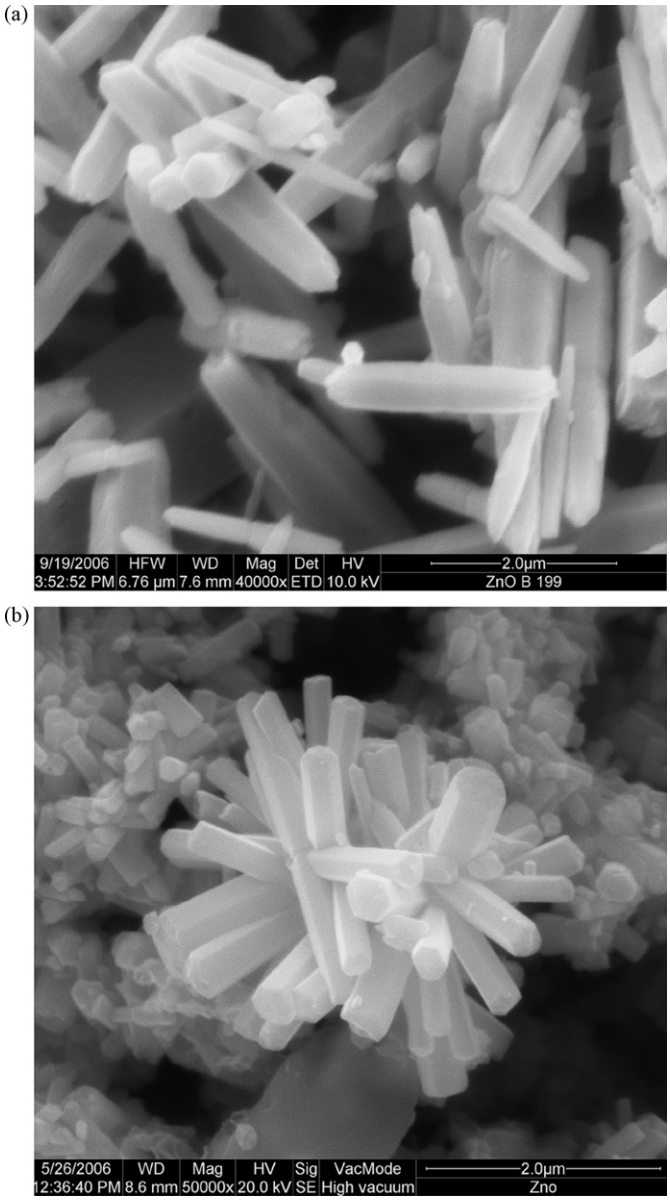

Fig. 1. Scanning electron micrographs of the ZnO nanorods with different orientations.

depicts the rod like nanostructures aligned in an irregular manner while they are found to be stacking at their tips thus showing typical structures where rods are arranged in the form of flowers (Fig. 1b) and this stacking phenomenon can be ascribed to the polar nature of the ZnO surface and the matching lattice structure. Moreover, these rods exhibit the hexagonal shape with diameter ranging from 200 nm to 500 nm and the length ranging from 500 nm to 3 μm (Fig. 1a).

Thereafter, the materials were characterized by X-ray diffraction technique in order to confirm the formation of ZnO and the same is apparently shown in Fig. 2. Bragg peaks appears at 31.775° 2θ, 34.425° 2θ, 36.275° 2θ and 47.625° 2θ which can be ascribed to the presence of (1 0 0), (0 0 2), (1 0 1) and (0 0 2) diffraction peaks. The data reveal the formation ZnO hexagonal shaped nanorods with wurtzite structure and the same was consistent with previously reported data [26]. On the other hand,

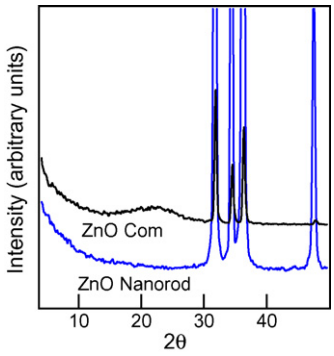

Fig. 2. X-ray diffraction patterns of the synthesized ZnO nanorods and the commercial bulk zinc oxide.

the ZnO nanorod samples were characterized also by FT-IR and the data have apparently shown the presence of surface hydroxyls as depicted by the appearance of IR absorption peaks at 3431 cm^{-1}, in addition to this, Zn–O absorption at 540 cm^{-1} is also observed.

After the characterization, obtained ZnO nanorod samples along with bulk ZnO were used to study the reaction with sulphur mustard (HD) at room temperature ($32 \pm 2\,^{\circ}C$). For this purpose, 100 μL of chloroform solution having 5 μL of HD was added to 300 mg of the above powder and the remaining HD was extracted by acetonitrile at periodic intervals of time until 48 h to study the kinetics of degradation on the surface of ZnO nanorods and bulk ZnO. For each time interval, the residual HD was extracted by using 5.0 mL of dichloromethane for five times in order to (each time 1 mL) ensure the complete extraction. Obtained solutions were quantitatively analyzed by calibrating the concentrations by using gas chromatograph equipped with flame ionization detector under isothermal conditions at 110 °C. As per GC data, sulphur mustard was eluted at 3.14 min for the reaction mixtures extracted from the ZnO NR and bulk ZnO, which were exposed to HD at kinetic intervals. Obtained kinetic data was plotted by taking $\log(a - x)$ on *Y*-axis and time on *X*-axis and the graph is depicted in Fig. 3. The two curves in the figure depict the kinetics of detoxification reaction of sulphur mustard on bulk ZnO and ZnO NR and each curve can be considered as two parts, i.e., the initial part of the reaction (faster) from 1 h to 12 h and final part of the reaction (steady state) from

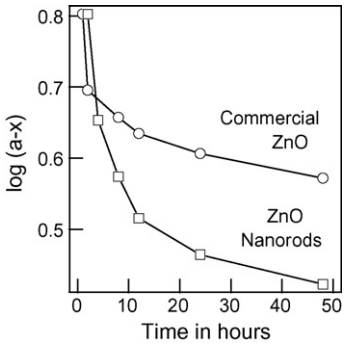

Fig. 3. Kinetics of degradation reactions of HD on the zinc oxide nanorods and the bulk zinc oxide.

12 h to 48 h. In the case of ZnO NR, initial part of the reaction is faster and exhibited a rate constant of 0.08175 h^{-1} and a half life of 8.48 h and the final part which can be considered as steady state exhibited a rate constant of 0.00566 h^{-1} and half life of 122.47 h. However, bulk ZnO exhibited a rate constant of 0.028 h^{-1} and half life of 24.75 h at initial stages (fast) and a rate constant of 0.00391 h^{-1} and a half life of 177.29 h at final stages (Table 1). The linearity of these individual segments indicates the first order behavior [21,22]. This observation can be attributed to the presence of more number of reactive sites in the ZnO nanorods. Although surface area of ZnO NR (52 m^2/g) is not much higher than commercial bulk ZnO (40 m^2/g), nanorods consist of larger number of reactive sites in the form of defects relative to the bulk ZnO, which enhances the rate of destructive reaction of HD on nanorods when compared with that of the bulk ZnO. The data also indicates that the HD molecules interact instantaneously with the unreacted active sites of the ZnO NR due to the high reactivity of the substrate, i.e., ZnO and the reach ability of HD molecules towards the unreacted surface from the bulk liquid. Moreover, the ZnO was treated with incipient amount of chloroform solution of HD, which facilitates the HD molecules to spread throughout the pore structure and reach the unreacted surface and cause the fast initial reaction. Once the liquid is spread and HD molecules come into the contact of the fresh surface of ZnO and react rapidly consuming the active surface. At this juncture, perhaps, the surface gets poisoned due the reaction of the surface with HD by forming the surface complexes. In order to understand this, we have exposed the sample with HD and after few hours of reaction, we have extracted the unreacted HD with meticulous amount of *n*-pentane and acetonitrile. Subsequently, we have characterized the sample by FT-IR after drying it. The typical IR absorption at 1222 cm^{-1}, 905 cm^{-1} and 720 cm^{-1} indicated the formation of surface complexes. Owing to this, the spreading of HD and the reaction with ZnO aggregates stops, however, the HD molecules can reach the unreacted surface by diffusion of evaporated molecules, thereby enabling the reaction to reach a steady state in approximately 24 h. Collectively, the spreading of liquid and evaporation, diffusion of HD molecules (vapour pressure 0.2 mmHg) could have influenced the pseudo first order reaction with a steady state and these results are consistent with reported ones.

Thereafter, the reaction mixtures were analyzed by GC–MS for the characterization of reaction products. Data illustrates the formation of several products. One of the spectra has *m*/*z* values at 122, 109, 104, 61 thus indicating the formation of thiodiglycol and another one has the *m*/*z* values at 140/142, 109, 91, 73, 61 and indicates the formation of hemi sulphur mustard thus emphasizing the role of hydrolysis reaction in the decontamination of HD thereby rendering it non-toxic. In addition to the hydrolysis product, we also have identified the products formed due to the elimination reaction like divinyl sulphide, vinyl chloro ethyl sulphide, and vinyl hydroxyl ethyl sulphide and shows the *m*/*z* values of 85, 71, 59 and 53; 122, 73, 60, 57 and 53; and 104, 73, 61, and 59, respectively. In addition to these reaction products residual HD was also observed with the *m*/*z* values at 158, 109, 73, 63 and 45. The reaction scheme of HD during hydrolysis and elimination reaction are also proposed and is

Table 1
Kinetic data of the detoxification reaction of sulphur mustard on zinc oxide nanorods and bulk zinc oxide

Type of sample	Initial part of the reaction (1–12 h)		Final part of the reaction (12–48 h)	
	Rate constant (h^{-1})	Half life (h)	Rate constant (h^{-1})	Half life (h)
Zinc oxide nanorods	0.08175	8.48	0.00566	122.47
Bulk zinc oxide	0.02800	24.75	0.00391	177.29

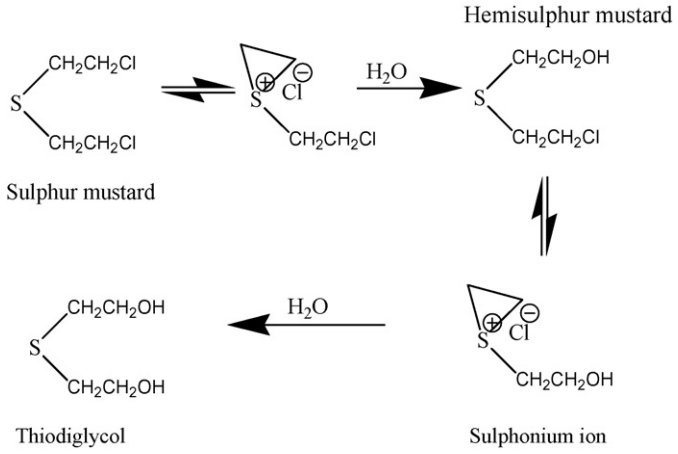

Scheme 1. Hydrolysis reactions of sulphur mustard occurring on the surface of ZnO nanorods.

depicted in Schemes 1 and 2. Most likely, sulphur mustard reacts with surface of ZnO to form sulphonium ion initially, soon after that, the sulphonium ion interacts with water molecules present within the ZnO nanostructures (no more water is added prior to the reaction) to form thiodiglycol and hemi sulphur mustard (Scheme 1). Moreover, sulphur mustard reacts with ZnO surface also by elimination reaction and releases hydrochloric acid and further yields the elimination products like divinyl sulphide, vinyl chloro ethyl sulphide and vinyl hydroxyl ethyl sulphide (Scheme 2). Released hydrochloric acid may react with ZnO surface and can form minute amounts of zinc chloride species thereby poisoning the active surface. In order to confirm the same, we have obtained the XRD data for the ZnO NR sample, which was treated with HD for 48 h. After the exposure, the sample was extensively washed with copious amounts of *n*-pentane and chloroform in order to remove the excess/residual HD and

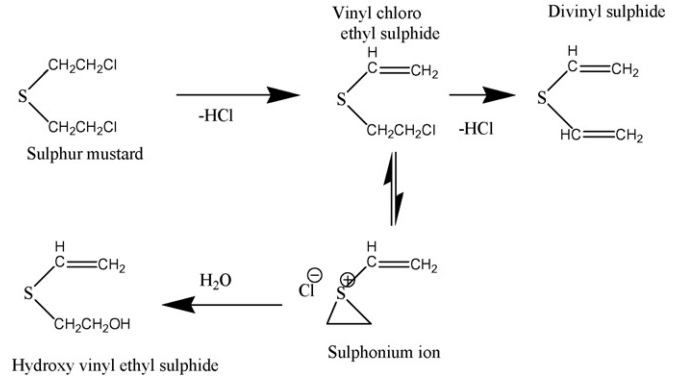

Scheme 2. Elimination and hydrolysis reactions of sulphur mustard occurring on the surface of ZnO nanorods.

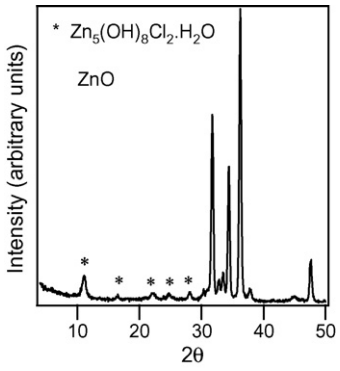

Fig. 4. X-ray diffraction pattern of the ZnO nanorods that are exposed to HD.

then the XRD data was obtained. The data shows the presence of peaks with low and noticeable intensity at 11.2, 16.5, 22, 24.8, 28.127 indicative of (0 0 3), (1 0 1), (1 0 4), (0 1 5) and (1 1 0) reflections in addition to the peaks characteristic of ZnO NR, thus depicting the formation $Zn_5(OH)_8Cl_2H_2O$ on the surface of ZnO nanorods due to the reaction of HCl released while HD reacted with ZnO NR surface (Fig. 4). However, hydrolysis reaction also occurred on the surface, which can be either attributed to surface hydroxyls or water molecules loosely bound to ZnO NR surface. In order to find out the amount of water in the ZnO NR, it was subjected to thermo gravimetric analysis. The data exhibited a weight loss of ~3% after heating up to 700 °C and it can be attributed to the small amount of water that was present on the surface either as water molecules or surface hydroxyls, whereas, commercial ZnO also exhibited only 3.5 wt.% loss of weight when heated up to 700 °C.

Precisely, the ZnO nanorods offer enough surface area and facilitate the adsorption and encapsulation of the HD molecules on the reactive sites present on the surface, most probably the surface hydroxyls will react with it rendering the hazardous agent to non-toxic. These results show that, the ZnO nanorods aggregates exhibit promising results on par with the existing solid decontamination systems such as nanosized MgO, Al_2O_3, etc. [1–12] and further emphasize the potentiality of ZnO NR for the decontamination of chemical warfare agents.

4. Conclusion

ZnO nanorods were synthesized by the hydrothermal method and characterized by SEM, XRD, FT-IR, TG, etc. Thereafter, they were used for studying the decontamination reaction with sulphur mustard, a chemical warfare agent. The results show that the ZnO nanorods are promising for the decontamination of sulphur mustard as it could destroy the agent by the pseudo first

order steady state reaction (hydrolysis and elimination) thereby promising the interesting CW decontamination applications.

Acknowledgements

We would like to thank Dr. F.V. Varghese, Dr. P.K. Gutch, A.N. Rao and Amit Saxena for useful suggestions.

References

[1] G.W. Wagner, L.R. Procell, R.J. O'Connor, M. Shekar, C.L. Carnes, P.N. Kapoor, K.J. Klabunde, J. Am. Chem. Soc. 123 (2001) 1636–1644.
[2] Y.-C. Yang, J.A. Baker, J.R. Ward, Chem. Rev. 92 (1992) 1729–1743.
[3] Y.-C. Yang, Chem. Ind. (1995) 334–337.
[4] K.J. Klabunde, Nanoscale Materials in Chemistry, 1st ed., Wiley Interscience Publishers, New York, 2004, p. 84.
[5] K.J. Klabunde, J. Stark, O. Koper, C. Mohs, D.G. Park, S. Decker, Y. Jiang, I. Lagadic, D. Zhang, J. Phys. Chem. 100 (1996) 12142.
[6] J.G. Ekerdt, K.J. Klabunde, J.R. Shapley, J.M. White, J.T. Yates, J. Phys. Chem. 92 (1988) 6182–6188.
[7] D.B. Mawhinney, J.A. Rossin, K. Gehart, J.T. Yates, Langmuir 15 (1999) 4789–4795.
[8] G.W. Wagner, P.W. Bartram, O. Koper, K.J. Klabunde, J. Phys. Chem. B 103 (1999) 3225–3228.
[9] G.W. Wagner, P.W. Bartram, ERDEC-TR-375, Aberdeen Proving Ground, MD, November, 1996.
[10] J.V. Stark, D.G. Park, I. Lagadic, K.J. Klabunde, Chem. Mater. 8 (1996) 1904–1912.
[11] P.W. Bartram, G.W. Wagner, US Patent No. 5,689,038, 18 November (1997).
[12] G.D. Sides, D.W. Mason, R.P. Seiders, Proceedings of the 1983 Scientific Conference on Chemical Defense Research, CRDC-SP-84014, Aberdeen Proving Ground, MD, October, 1984, pp. 285–291.
[13] G.W. Wagner, P.W. Bartram, J. Mol. Catal. A: Chem. 111 (1996) 175–180.
[14] G.W. Wagner, P.W. Bartram, J. Mol. Catal. A: Chem. 99 (1995) 175–181.
[15] G.W. Wagner, O. Koper, E. Lucas, S. Decker, K.J. Klabunde, J. Phys. Chem. B 104 (2000) 5118–5123.
[16] N.W. Emanetoglu, C. Gorla, Y. Liu, S. Liang, Y. Lu, Mater. Sci. Semicond. Process. 2 (1999) 247.
[17] Y. Chen, D. Bagnall, T. Yao, Mater. Sci. Eng. B 75 (2000) 190.
[18] N. Saito, H. Haneda, T. Sekiguchi, N. Ohashi, I. Sakaguchi, K. Koumoto, Adv. Mater. 14 (2002) 418.
[19] S. Liang, H. Sheng, Y. Liu, Z. Hio, Y. Lu, H. Shen, J. Cryst. Growth 225 (2001) 110.
[20] J.Y. Lee, Y.S. Choi, J.H. Kim, M.O. Park, S. Im, Thin Solid Films 403 (2002) 533.
[21] M.H. Koch, P.Y. Timbrell, R.N. Lamb, Semicond. Sci. Technol. 10 (1995) 1523.
[22] Y. Lin, Z. Zhang, Z. Tang, F. Yuan, J. Li, Adv. Mater. Opt. Electron. 9 (1999) 205.
[23] N. Golego, S.A. Studenkin, M. Cocivera, J. Electrochem. Soc. 147 (2000) 1592.
[24] B. Blajeni-Aurian, M.M. Boucher, Langmuir 5 (1989) 170.
[25] S.M. Kanan, C.P. Tripp, Langmuir 17 (2001) 2213.
[26] Q. Li, V. Kumar, Y. Li, H. Zhang, T.J. Marks, R.P.H. Chang, Chem. Mater. 17 (2005) 1001.